

A mid-twentieth century reduction in tropical upwelling inferred from coralline trace element proxies

Matthew K. Reuer^{a,*}, Edward A. Boyle^b, Julia E. Cole^c

^a MIT/WHOI Joint Program in Oceanography, E34-200, Massachusetts Institute of Technology, Cambridge, MA 02139, USA

^b Department of Earth, Atmospheric, and Planetary Sciences, E34-200, Massachusetts Institute of Technology, Cambridge, MA 02139, USA

^c Department of Geosciences, The University of Arizona, Gould-Simpson Building, 1040 E. Fourth Street, Tucson, AZ 85721-0077, USA

Received 5 November 2002; received in revised form 12 March 2003; accepted 14 March 2003

Abstract

The Cariaco Basin is an important archive of past climate variability given its response to inter- and extratropical climate forcing and the accumulation of annually laminated sediments within an anoxic water column. This study presents high-resolution surface coral trace element records (*Montastrea annularis* and *Siderastrea siderea*) from Isla Tortuga, Venezuela, located within the upwelling center of this region. A two-fold reduction in Cd/Ca ratios (3.5–1.7 nmol/mol) is observed from 1946 to 1952 with no concurrent shift in Ba/Ca ratios. This reduction agrees with the hydrographic distribution of dissolved cadmium and barium and their expected response to upwelling. Significant anthropogenic variability is also observed from Pb/Ca analysis, observing three lead maxima since 1920. Kinetic control of trace element ratios is inferred from an interspecies comparison of Cd/Ca and Ba/Ca ratios (consistent with the Sr/Ca kinetic artifact), but these artifacts are smaller than the environmental signal and do not explain the Cd/Ca transition. The trace element records agree with historical climate data and differ from sedimentary faunal abundance records, suggesting a linear response to North Atlantic extratropical forcing cannot account for the observed historical variability in this region.

© 2003 Elsevier Science B.V. All rights reserved.

Keywords: trace elements; Cariaco Basin; coral reefs; paleoclimatology; cadmium; barium

1. Introduction

The tropical North Atlantic exhibits significant interdecadal climate variability as determined by

historical climate records, paleoclimate proxy data, and coupled ocean–atmosphere general circulation models [1–5]. The timing and magnitude of its Holocene variability have been addressed by multiple sedimentary proxies from the anoxic Cariaco Basin ([4,6–8] and references therein). The inferred variability from the sedimentary records can be tested by high-resolution surface coral records, providing an annually resolved, multi-decadal comparison. This study presents surface

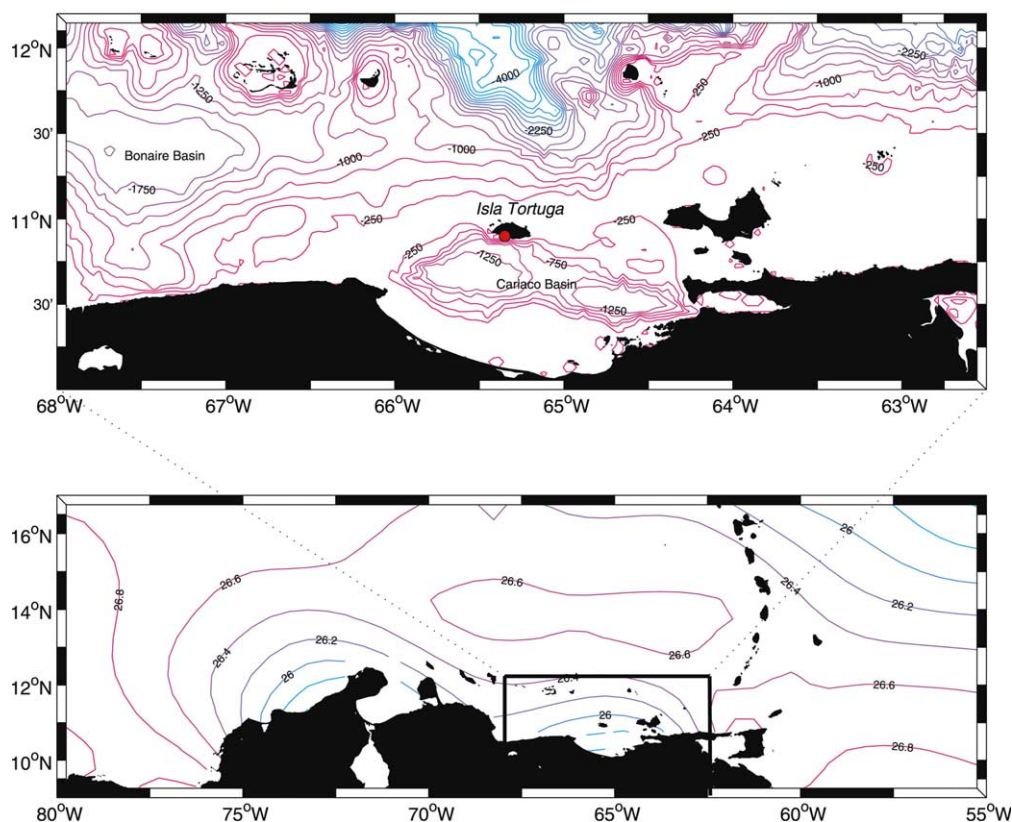
* Corresponding author. Fax: +1-609-258-1724.

E-mail addresses: mreuer@princeton.edu (M.K. Reuer), eaboyle@mit.edu (E.A. Boyle), jcole@geo.arizona.edu (J.E. Cole).

coral trace element records from the Cariaco Basin upwelling zone, demonstrating trace element variability consistent with historical climate records and providing new evidence for a century-scale reduction in tropical upwelling.

The Cariaco Basin is an important tropical paleoclimate archive based on its response to regional climate forcing and the annual accumulation of sedimentary laminae. Coastal upwelling in this region is determined by the position of the Intertropical Convergence Zone (ITCZ), the associated North Atlantic wind stress anomalies, and subsequent northward Ekman transport. Fig. 1 shows the location and bathymetry of the Cariaco Basin

and the reduction in regional sea surface temperatures (SST) due to upwelling. The rapid accumulation ($> 100 \text{ cm kyr}^{-1}$) of laminated sediments within an anoxic water column creates a high-resolution, annually resolved sedimentary record [4,6,9]. Geochemical and micropaleontological proxy records have been developed from this region, including planktonic $\Delta^{14}\text{C}$ [10,11], sedimentary gray-scale records [6], faunal abundance records [4,7], planktonic $\delta^{18}\text{O}$ [12], and sedimentary major elements [8]. Of these results, the faunal abundance record of Black et al. [7] resolves decadal historical variability. Based on the abundance of the planktonic foraminifer *Globigerina*



bulloides with respect to sediment mass, an anti-correlation (ca. $r = -0.8$) was observed with North Atlantic SST anomalies (at 50°N, 35°W). This result suggests a linear, coupled response between subtropical–subpolar SSTs, northeasterly trade wind intensity, and coastal upwelling on decadal time scales.

Historical climate observations from the Cariaco Basin provide a first-order constraint on past variability, including the COADS SST and marine air temperature (MAT) observations shown in Fig. 2 [13]. This data set was selected for its $2 \times 2^\circ$ observations from 1859 to 1992 in the Cariaco Basin region (centered on 11°N, 65°W); $5 \times 5^\circ$ grids or above do not adequately resolve regional upwelling. Historical climate records include two well-known artifacts: bias resulting from discrepant measurement techniques and aliasing due to inadequate annual observations. For example, early twentieth century SST estimates were approximately 0.3–0.7°C too low due to the container type (wooden, canvas, or insulated buckets), the measurement location (sunlight or shade), and the vessel speed (sail or steam [14]). Using historical land air temperature, MAT, and SST data, Jones et al. [14] calculated the following historical SST biases for the northern hemisphere: +0.08°C (1861–1889), –0.49°C (1903–1941), +0.07°C (1942–1945), and –0.02°C (1946–1979). Two simple techniques were utilized to address this problem. First, the measured SST variability was compared to the estimated bias for the time interval of interest (–0.49°C from 1903 to 1941 [14]), neglecting interannual variability below this limit. Second, temperature differences were calculated between the Cariaco Basin and a Caribbean, non-upwelling domain (13°N, 65°W). Assuming consistent historical SST measurements, the temperature gradient should reflect the relative upwelling intensity within the Cariaco Basin. Finally, the MAT data are also considered, based on their lower estimated measurement bias (0.23°C from 1903 to 1941 [14]). All three mean annual historical climate records show negative mean annual temperature anomalies from approximately 1920 to 1943, followed by positive anomalies from 1943 to 1988 (Fig. 2). From the high-resolution COADS SST record (not shown),

SST anomalies less than -3°C were observed in 7 years from 1920 to 1950 (1922, 1923, 1926, 1936, 1937, 1939, 1946), whereas only 2 years from 1950 to 1995 (1957, 1992) were of equivalent magnitude. Both MAT and SST results thus suggest a reduction in Cariaco Basin upwelling during the 20th century. To test this hypothesis, trace element ratios have been measured in the surface corals *Montastrea annularis* and *Siderastrea sidera*, measuring multiple elements to best isolate the upwelling signal.

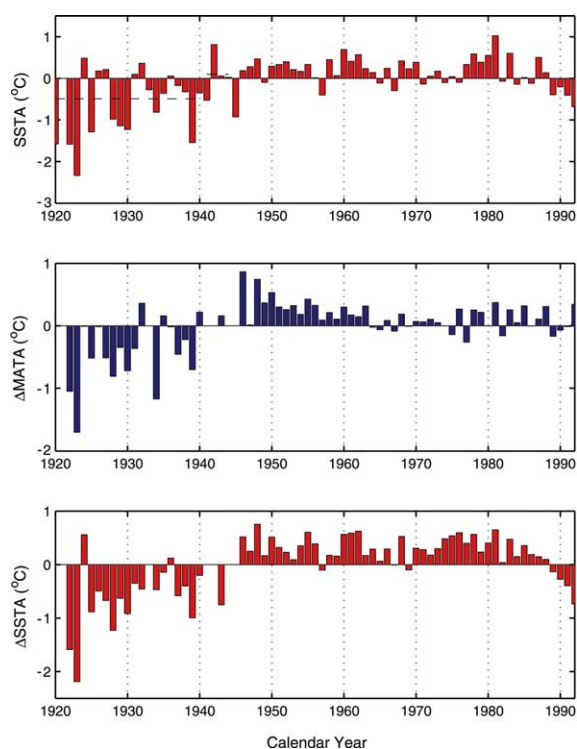


Fig. 2. Historical climate records from the Cariaco Basin, COADS data series ($2 \times 2^\circ$, 1859–1992). All anomalies were calculated with respect to the 1920–1992 interval. The upper panel shows the SST anomaly (SSTA) record from the 11°N, 65°W grid point. The dashed lines reflect the historical SST measurement bias from Jones et al. [14] (see text for discussion), and note the Cariaco Basin anomalies from 1920 to 1945 cannot be explained by measurement bias alone. The middle and lower panels show the MAT and SST difference anomalies between the 13°N and 11°N grid points (see text for discussion). Correlation ($r = 0.846$) between the SSTA and ΔSSTA results suggests the Cariaco grid point determines the temperature difference.

The utility of surface coral¹ trace element proxies is supported by multiple calibration studies, and a brief synopsis is provided. First, Shen et al. [15] and Lea et al. [16] demonstrated Cd/Ca, Ba/Ca, and Pb/Ca variability consistent with anthropogenic emissions and equatorial Pacific SSTs, suggesting elemental ratios quantitatively reflect past surface ocean chemistry. Several additional trace elements, including manganese [17,18], uranium [19,20], and the rare earth elements [21] have also been calibrated for surface corals, and down-core trace element correlations are observed on seasonal to centennial time scales [22,23]. Successful calibration of these elements likely reflects limited trace element discrimination during surface coral calcification, and this discrimination can be quantified by the Henderson–Kracek partition coefficient [24]:

$$D_p = (X/Ca)_{\text{coral}} / (X/Ca)_{\text{seawater}}$$

where X corresponds to the chemical species of interest and $D_p > 1$ implies preferential precipitation from the aqueous phase. A multi-element compilation shown in Fig. 3 demonstrates: (1) most elements exhibit partition coefficients close to unity; (2) departures from this trend likely result from steric effects (where the substituent ionic radius greatly differs from Ca^{2+} or CO_3^{2-}), charge imbalance, or biological uptake; and (3) surface coral elemental ratios show a wide concentration range, exceeding 10 orders of magnitude. Given minor discrimination of trace elements relative to Ca^{2+} in coral aragonite, previous calibrations suggest surface corals faithfully record past variations in surface ocean chemistry.

Trace element variability in surface corals might also include significant kinetic artifacts similar to the growth rate dependence reported by de Villiers et al. [25,26] for Sr/Ca ratios. One example of trace element kinetic artifacts is shown in Reuer [27], where systematic Pb/Ca offsets were observed between contemporaneous *Diploria* records from North Rock, Bermuda. For this study,

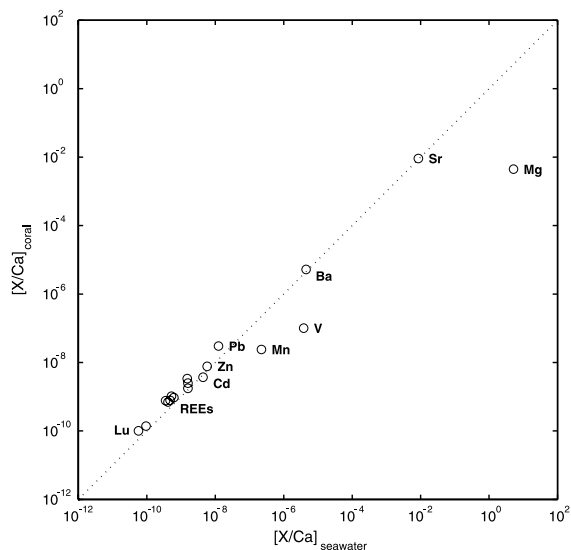


Fig. 3. Element/calcium (X/Ca) ratios for surface corals and seawater. All data and associated references are given in Reuer [27], and the label ‘REEs’ corresponds to the rare earth elements. The Y -axis reflects element/calcium ratios for surface corals, the X -axis denotes the corresponding seawater ratios, and the dashed line reflects a partition coefficient (D_p) of 1. The points above the line (e.g. Pb, Lu) correspond to preferential elemental uptake by surface corals, whereas the points below the line (e.g. Mg, Mn, V) correspond to exclusion. Note the observed exclusion of Mn^{2+} , V^{4+} , and Mg^{2+} in coral aragonite, a possible consequence of reduced ionic radii relative to Ca^{2+} ($\text{Mg}^{2+} = 0.89 \text{ \AA}$, $\text{Mn}^{2+} = 0.96 \text{ \AA}$, $\text{Ca}^{2+} = 1.12 \text{ \AA}$, from Shannon [75]), charge imbalance (V^{4+}), or biological uptake by coral symbionts (Mg, Mn, or V).

large kinetic effects were observed for the slowly growing *S. siderea* relative to *M. annularis* (see below). Consequently, the *M. annularis* record will be the focus of this study. Trace element records cannot be completely interpreted without considering these possible artifacts, and a universal calibration cannot be applied to individual trace element records.

Given this proxy system, what elemental variability is expected within the Cariaco Basin, particularly for cadmium and barium? To evaluate this response, the dissolved cadmium [28] and barium [29] hydrographic profiles are shown in Fig. 4. The greater increase in cadmium concentrations (258%) versus barium (2%) is evident within the upper 150 m, resulting from the established shallower regeneration of labile phytodetritus [30,31]

¹ In this paper the general term ‘surface corals’ refers to hermatypic (reef-building), zooxanthellate (symbiont-bearing), scleractinian corals (subclass Zoantharia, class Anthozoa, subphylum Cnidaria).

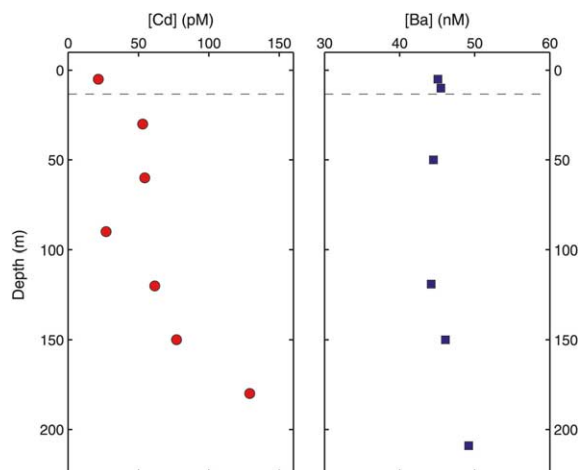


Fig. 4. Mixed-layer dissolved cadmium and barium profiles from the Cariaco Basin: Jacobs et al. [28] and Falkner et al. [29], respectively. For comparison the climatological mixed-layer depth is shown for the sample collection period (November) as dashed lines [76]. Between 5 and 150 m, the linear concentration gradients are 0.383 pM m^{-1} for $d[\text{Cd}]/dz$ and 0.007 nM m^{-1} for $d[\text{Ba}]/dz$. These profiles support cadmium's enhanced sensitivity to upwelling variations in the Cariaco Basin.

relative to biogenic barite [32–34]. Assuming upwelling extends to the base of the seasonal pycnocline (ca. 150 m [35]), a greater change in cadmium concentrations would be expected relative to barium. This response, however, is likely non-conservative and complex, including biological uptake of upwelled cadmium, the admixture of upper thermocline water with other nutrient-depleted surface water masses, and possible island effect upwelling near reef sites. A key assumption of this study is elevated mixed-layer cadmium concentrations simply reflect intensified upwelling.

A second primary trace element source is regional fluvial inputs. The Orinoco River is the greatest expected input to the southern Caribbean, with greatest discharge in late boreal fall corresponding to the precipitation maximum associated with the ITCZ. Seasonal fluvial inputs are best demonstrated by satellite ocean color observations, where Orinoco and Amazon river nutrient fluxes increase pigment and colored dissolved organic matter concentrations in areally extensive plumes within the southern Caribbean ($> 3 \times 10^5 \text{ km}^2$ [36–38]). Given elevated cadmium

and barium concentrations measured from the Orinoco and Changjiang rivers ($\text{Cd} \approx 700 \text{ pM}$, $\text{Ba} \approx 225 \text{ nM}$ [39]) and their subsequent particulate desorption in estuaries, a fluvial input is hypothesized. Like upwelling variability, any resulting change in trace element concentrations is complex, dependent upon seawater dilution of the river plume, its advection into the Cariaco Basin, and subsequent biological removal of the trace element signal. Given the entrainment of the Orinoco–Amazon plume within the westward, 13°N Caribbean Current jet (as suggested by satellite chlorophyll images, Hernández-Guerra and Joyce [40] and references therein), the influence of the large South American rivers might be less than local, low-discharge systems.

2. Methods

The methods utilized for this study include several established techniques [41] updated for current inductively coupled plasma mass spectrometry (ICP-MS) instrumentation. Complete details regarding the collection, sampling, and analysis of the coral cores are provided in Reuer [27]. Here a brief description is given, followed by discussion of the Cariaco Basin physiography, hydrography, and climatology.

2.1. Analytical methodology

Surface coral cores were collected from two sites along the southern coast of Isla Tortuga, Venezuela, in 1996 and 1998 (Fig. 1). Water depths (as sea surface to the colony top) ranged from approximately 2 to 3 m at the time of sampling. Coral cores were collected with an underwater hydraulic drill and steel carbide core barrel, manually stabilizing the drill system and removing coral fragments with pressurized seawater. The oriented core sections were then cut into 1 cm width slabs with a water-cooled tile saw, using a steel carbide blade. Following core collection and sectioning, the dissepiment orientation was determined by X-radiography, measuring annual extension rates, growth axis position, and any section breaks. Samples were collected along the

primary growth axis with a diamond-coated steel wire (130.2×0.08 mm, Crystalite), and the coral slab only contacted polycarbonate surfaces during sampling. Coarse sampling resolution is required for adequate sample masses (approximately 250 mg), resulting in five to six samples per year for *M. annularis* and two samples per year for *S. siderea*. This coarse resolution will mute the amplitude of the seasonal cycle required for full-amplitude monthly estimates. Prior to analysis, the surface corals were cleaned with a modified method of Shen and Boyle [41] described in Reuer [27], utilizing two primary cleaning sequences of both coarse aragonite fragments and a 280–700 μm size fraction. Each cleaning sequence included oxidants (0.1 N NaOH–15% H_2O_2), reductants (citric acid–hydrazine), and dilute acid (0.1 N HNO_3), using ultrasonic cleaning and elevated reaction temperatures ($T > 90^\circ\text{C}$) to quantitatively remove organic and oxide contaminants.

The analytical methods used in this study include graphite furnace atomic absorption spectrophotometry (GFAAS) and isotope dilution ICP-MS (ID-ICP-MS), and all duplicate analyses were completed on homogenized splits of individual samples. First, cadmium concentrations were determined via GFAAS, preconcentrating cadmium from the CaCO_3 matrix with Co-APDC coprecipitation [41,42]. The reaction was completed at pH 10.7 via distilled NH_3 additions, observing elevated and consistent recoveries ($95.2 \pm 3.0\%$, $n=16$) relative to pH 0.8 (77.3% , $n=4$). This result likely reflects diminished H^+ competition for the APDC complex, consistent with the Zn^{2+} and Fe^{2+} observations of Boyle and Edmond [42]. Lead and barium concentrations were determined by ID-ICP-MS (VG PlasmaQuad 2+), spiking sample solutions with well-characterized ^{135}Ba and ^{204}Pb spike standards [43,44]. All spikes were repeatedly calibrated with gravimetric ICP-MS standards (J.T. Baker) prior to use. Standard corrections for instrumental backgrounds, isobaric interferences (^{204}Hg), and procedural blanks were utilized.

Core chronologies were based solely on the annual density couplet common to *M. annularis* (see [45]) and *S. siderea*. As the focus of this study, a representative *M. annularis* section is shown in

Fig. 5. Several limitations of this preliminary chronology must be emphasized based on the limited core material collected from Isla Tortuga. First, spurious age assignments can result from

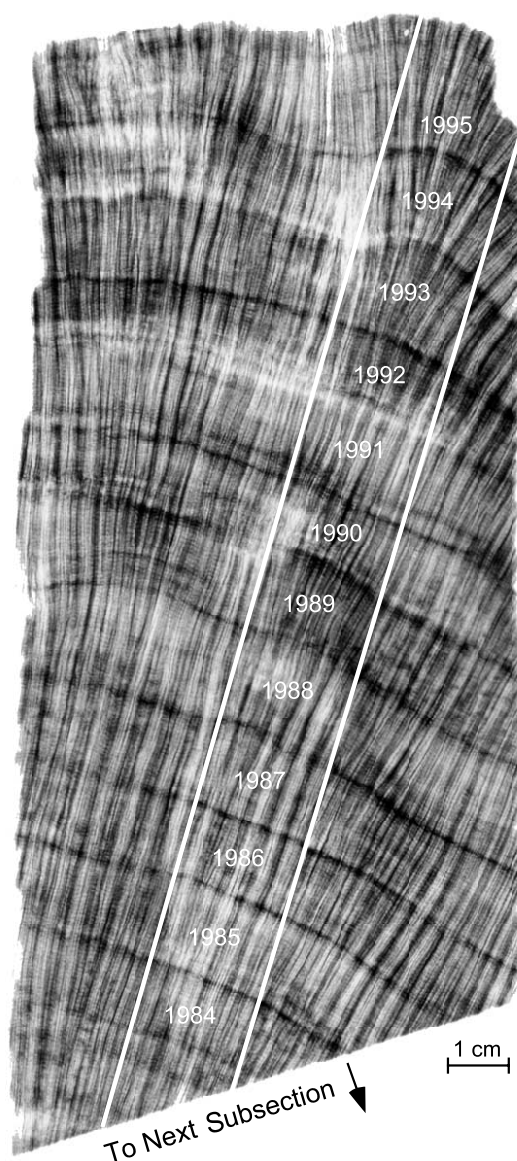


Fig. 5. X-radiograph positive of a characteristic *M. annularis* section from Isla Tortuga, the corresponding age assignments, and sampling trajectory. Note the alternating dark (low-density) and light (high-density) horizontal dissepiments with an annual extension rate of 13 mm yr^{-1} . The vertical calices correspond to aragonite deposition by individual polyps. The image scale bar is 1 cm.

faint or duplicate density banding patterns common to *M. annularis* dissepiments; questionable sections were assumed to have annual extension rates comparable to the 13 mm yr^{-1} mean. Second, three section breaks occur within this core (at the assigned ages of 1923, 1939, and 1964) due to bioerosion and drilling losses, and stratigraphic continuity has been assumed between each section. The resulting absolute chronological errors will be too recent, while relative ages within individual sections will be correct. Despite these limitations, reasonable chronological agreement is observed between the Cd/Ca and SST variability (see below): an offset of three years was determined between the final positive Cd/Ca anomaly (1949) and the corresponding negative SST anomaly (1946). Most importantly, the emphasis of this study is the centennial trace element variability and its generalized comparison with historical climate records. The exact timing of the inferred variability will be determined by multiple, overlapping cores from a single colony and high-resolution stable isotope analyses.

2.2. Cariaco Basin hydrography

Before presenting the trace element results, the regional hydrography and climatology must be considered. The Cariaco Basin represents two extensional sub-basins bounded to the south by the South American continent and to the north by the Tortuga Bank [9]. The high-resolution Smith and Sandwell [46] bathymetry is shown in Fig. 1. The shallow Tortuga Bank is transected by the Canal Centinela to the northwest (116 m) and the Canal de la Tortuga to the northeast (195 m) [35], restricting intermediate water flow above 200 m. This bathymetry results in uniform temperature (16.9°C) and salinity (36.2‰) from 300 to 1390 m [9]. Low intermediate water ventilation, high integrated primary production rates ($540\text{--}690 \text{ gC m}^{-2} \text{ yr}^{-1}$, [35]), and subsequent organic matter degradation [47] creates the well-known water column anoxia. The shallow mixed layer and upper thermocline of the Cariaco Basin are affected by coastal upwelling (late boreal winter to spring) resulting from Ekman divergence forced by the northeasterly trade winds (Fig. 1). South Ameri-

can coastal upwelling, the associated surface currents, and their temperature–salinity characteristics are complex [40], including two distinct upwelling centers near northern Venezuela and Colombia, westerly countercurrents south of the Caribbean Current, and salinity minima due to fall freshwater influxes from the Orinoco and Amazon rivers.

2.3. Tropical North Atlantic climatology

The climate of the tropical North Atlantic is governed by the seasonal meridional position of the ITCZ (see [48,49]). During late boreal winter (March–April), the ITCZ reaches its southernmost extreme, associated with SST and precipitation maxima in the tropical South Atlantic and a hemispheric SST difference of -4 to -5°C (N–S domains [50]). EOF analysis by Nobre and Shukla [51] demonstrated SST anomalies in this region are preceded by wind stress anomalies two months in advance, suggesting a SST response to trade wind forcing. In boreal summer, positive SST anomalies in the tropical North Atlantic result from lower wind stress and latent heat fluxes, reversing the north–south SST gradient, shifting the ITCZ to the north, and increasing tropical North Atlantic precipitation. The mean position and dynamics of the ITCZ are thus governed by coupled ocean–atmosphere variability [52], affecting SST distributions in the tropical Atlantic and precipitation variability in the African Sahel and Brazilian Nordeste [1,51,53,54].

Multiple climate forcing mechanisms have been developed to explain tropical North Atlantic variability. Coupled air–sea interactions are an important mechanism in this region, associated with a SST ‘dipole’ between the northern and southern tropical Atlantic [3,5]. The persistence of this feature is currently debated [5,55,56]; however, northern and southern tropical Atlantic SSTs are significantly anti-correlated on decadal time scales. For example, Chang et al. [5] observed a significant dipole SST pattern in the first leading mode of a joint (surface wind and SST) singular value decomposition analysis, and model results have shown a decadal SST response between the northern and southern tropical Atlantic

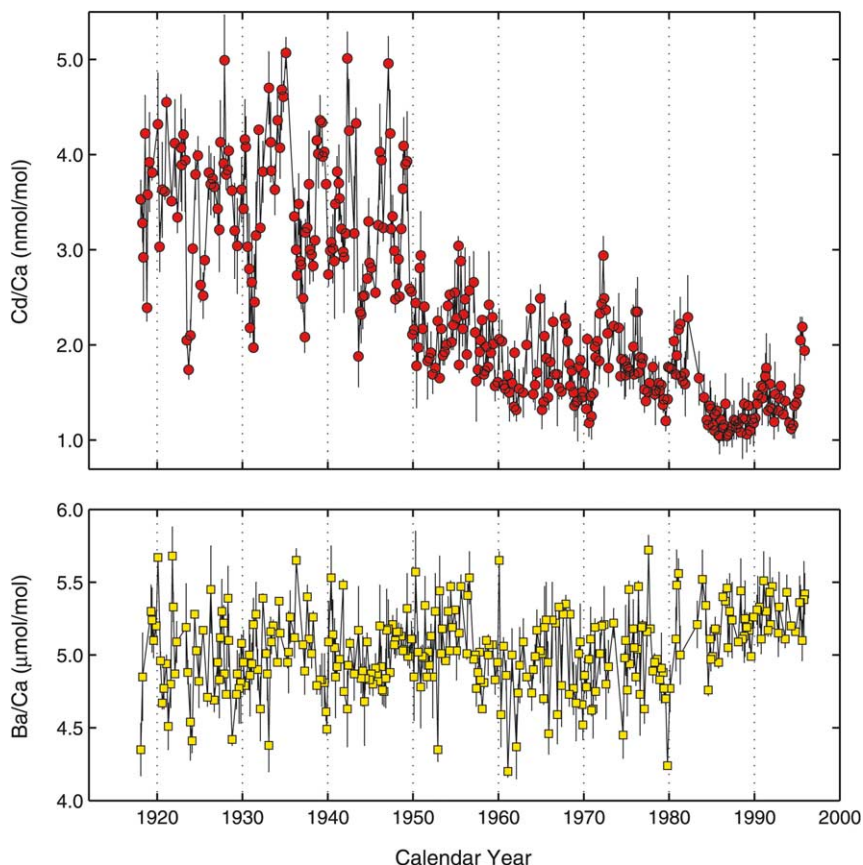


Fig. 6. Isla Tortuga raw Cd/Ca and Ba/Ca records. These results reflect duplicate sample analyses of a single *M. annularis* core. The upper panel shows the Cd/Ca ratios (in nmol/mol), and the lower panel shows the Ba/Ca record (in $\mu\text{mol/mol}$). Error bars are 2σ calculated from sample replicates, including cleaning and analytical uncertainties. Note the Cd/Ca transition at 1950 and no corresponding shift in Ba/Ca. A systematic increase in Ba/Ca is also observed at 1981.

with both stochastic [5] and climatological [57] wind stress forcing. Coupled equatorial interactions similar to the Pacific El Niño–Southern Oscillation (ENSO) phenomena have been reported [58–60], although their recurrence and magnitude are less than their Pacific counterpart. Finally, extra- and intratropical forcing, including NAO [61] and ENSO [51,56,62] coupling, have been demonstrated, modulating the ‘dipole’ dynamics via atmospheric forcing.

3. Results and discussion

The principal trace element records from Isla Tortuga, Venezuela are shown in Fig. 6. The

Cd/Ca and Ba/Ca data are also presented in Fig. 7 as mean annual anomalies (calculated with respect to the entire record length) and annual amplitudes. A two-fold Cd/Ca reduction is observed between 1920–1950 (3.48 nmol/mol) and 1950–1995 (1.73 nmol/mol), occurring between 1946 and 1952. The Ba/Ca ratio does not show a comparable transition across this interval, with the Ba/Ca standard deviation equal to 0.35 $\mu\text{mol/mol}$ (2σ). The Cd/Ca reduction is synchronous with a decreased annual amplitude, whereas no comparable Ba/Ca modulation is observed. Comparison between the Cd/Ca and Ba/Ca results and the trace element hydrographic distributions shown in Fig. 4 supports a possible mid-20th century reduction in coastal upwelling.

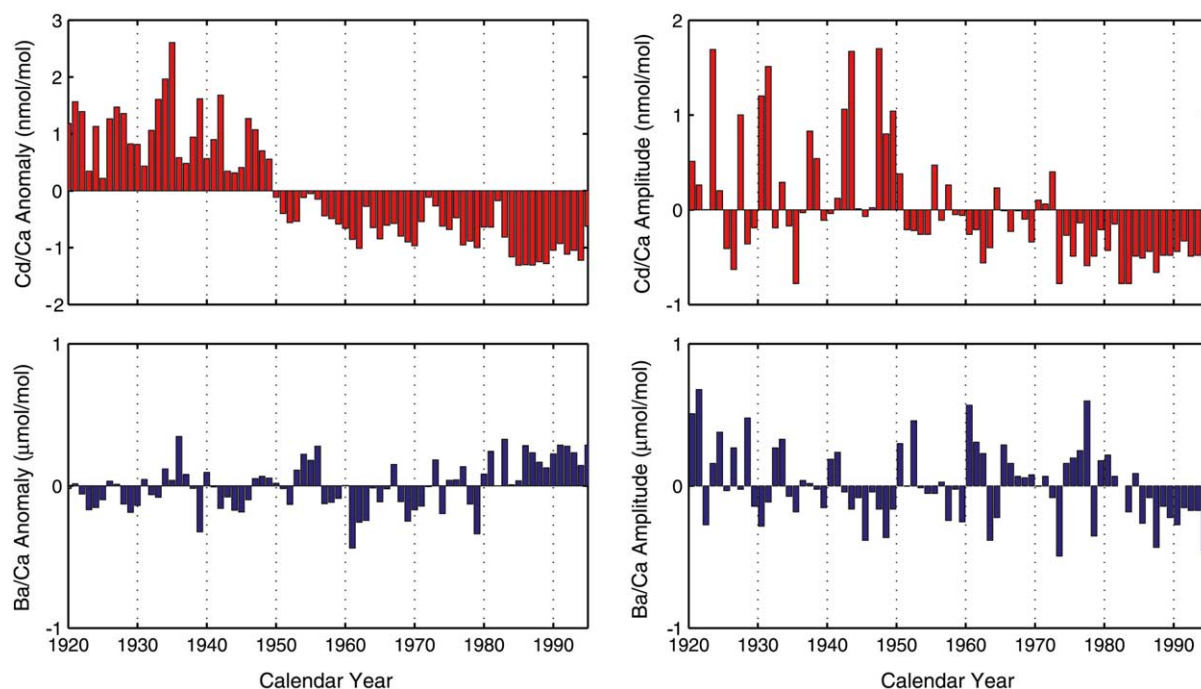


Fig. 7. Left panels: Isla Tortuga mean annual Cd/Ca and Ba/Ca anomalies. The anomalies are calculated with respect to the complete record length (1918–1996). Note the predominant Cd/Ca transition at 1950 and the diminished mean annual Ba/Ca variability. Right panels: Isla Tortuga Cd/Ca (nmol/mol) and Ba/Ca ($\mu\text{mol/mol}$) annual amplitude anomalies. Note the dampened Cd/Ca amplitude after 1950 and no comparable shift in Ba/Ca.

3.1. Surface coral trace element artifacts

Before interpreting these results, the known artifacts influencing surface coral trace element ratios must be addressed. The first consideration is

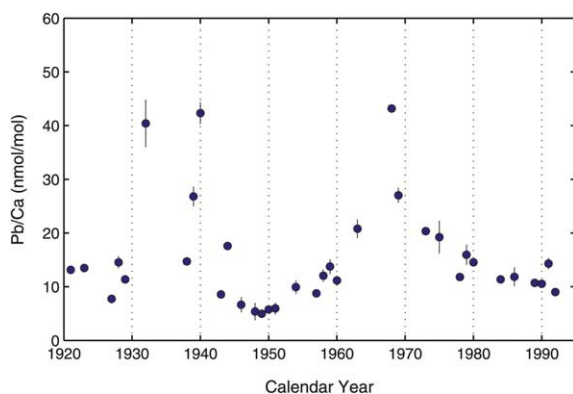


Fig. 8. Cariaco Basin Pb/Ca record: Isla Tortuga. Note the Pb/Ca maxima (1932, 1940, and 1968) and no elemental transition at 1950. Error bars are 2σ from sample duplicates.

the coral cleaning technique, isolating seawater-derived trace elements associated with the aragonite lattice [41]. One useful test is the signal-to-noise ratio between sample replicates and the signal of interest, assuming contaminated replicates will not be equal. The magnitude of the mid-century shift is 1.8 nmol/mol. With a mean replicate 2σ standard deviation of 0.2 nmol/mol, the S/N ratio (9) suggests the observed signal is not a contamination artifact. The Pb/Ca record (Fig. 8) supports this hypothesis with no observed Pb/Ca transition and the established Pb/Ca response to sample contamination [41]. The mean Cariaco Basin Cd/Ca ratio (2.37 nmol/mol) can also be compared with previous analyses from Bermuda (0.44 nmol/mol [63])² and the Galápagos (5.30 nmol/

² This estimate was determined from the 1867–1899 Cd/Ca mean to minimize potential anthropogenic cadmium contributions to North Rock, Bermuda.

mol [22]). Because these ratios are consistent with the mean annual mixed-layer phosphate concentrations at each site (0.321, 0.088 and 0.608 μM [64]), the mean Cariaco Basin Cd/Ca ratio agrees with previous, independent trace element analyses.

3.2. Kinetic artifacts

A second possible surface coral artifact is kinetic trace element fractionation, as suggested by the Sr/Ca calibrations of de Villiers et al. [25,26] and Cohen et al. [65]. Reduced coral extension rates ($14\text{--}6\text{ mm yr}^{-1}$) resulted in elevated Sr/Ca ratios (ca. $9.08\text{--}9.22\text{ mmol/mol}$ at 1980) for the Pacific species *Pavona clavus*. To address this issue for cadmium and barium, we have analyzed two coral species with different extension rates, ranging from 7 mm yr^{-1} for *S. siderea* to 13 mm yr^{-1} for *M. annularis*. The results are shown in Fig. 9, observing consistently higher and variable trace element ratios for *S. siderea*. Interspecies differ-

ences for Ba/Ca ($6.0\text{ }\mu\text{mol/mol}$) and Cd/Ca (2.3 nmol/mol) are of equal magnitude to the observed range from the Cariaco Basin records. Most importantly, the instantaneous calcification rate must be measured for a quantitative comparison, and other interspecies differences (e.g. colony topography) cannot be discounted without a systematic trace element calibration.

The results shown in Fig. 9 suggest kinetic artifacts will affect both the absolute elemental ratio between reef colonies and the relative variability within an individual record. For example, the Ba/Ca range (1976–1994) is from $0.66\text{ }\mu\text{mol/mol}$ for *M. annularis* to $4.10\text{ }\mu\text{mol/mol}$ for *S. siderea*. Because the *S. siderea* colony was not located at the exact same site, some of the elemental differences might reflect local variability. High-resolution seawater cadmium and barium measurements at these reef sites, however, presently do not exist. Elemental contamination from the dense trabeculae of *S. siderea* might also contribute to the elevated noise observed in this record.

Can the Isla Tortuga Cd/Ca transition be explained by this significant kinetic artifact? Three observations oppose this hypothesis. First, no corresponding Ba/Ca reduction is observed as expected from the Cd/Ca and Ba/Ca kinetic effect (Fig. 6). Second, no significant difference in annual extension rate was observed across this interval: the 1920–1950 ($13.3 \pm 4.0\text{ mm yr}^{-1}$) and 1950–1995 ($13.3 \pm 4.3\text{ mm yr}^{-1}$) averages are equal within the 95% confidence interval. Third, the environmental Cd/Ca variability (approximately 5 nmol/mol for Cd/Ca) is still larger than the artifact implied from the *S. siderea* comparison: an extension rate reduction to 7 mm yr^{-1} will increase Cd/Ca by 2 nmol/mol . Kinetic effects are significant determinants of coralline trace element ratios, but they cannot explain the mid-century Cd/Ca reduction.

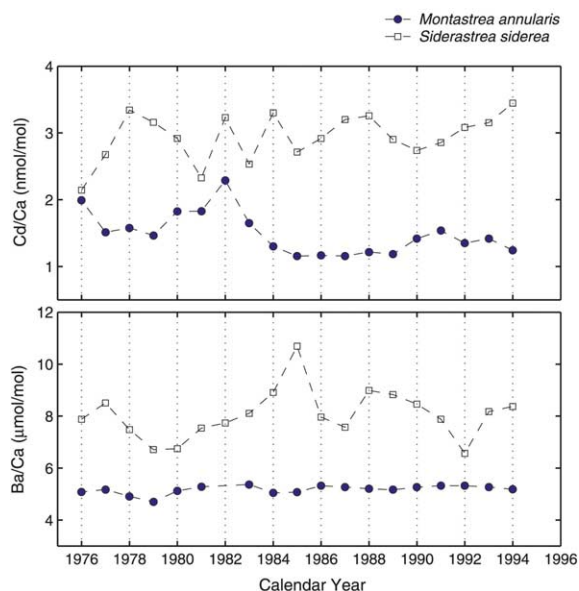


Fig. 9. Trace element interspecies comparison (*S. siderea* and *M. annularis*), including Cd/Ca (nmol/mol, upper panel) and Ba/Ca ($\mu\text{mol/mol}$, lower panel). The *S. siderea* data are shown as open squares, and the *M. annularis* results are given as closed circles. All results are shown as mean annual elemental ratios to account for sampling resolution differences, and the time interval is from 1976 to 1994.

3.3. Anthropogenic artifacts

Finally, anthropogenic cadmium influxes represent another possible artifact given possible emissions from metal smelting, chemical processing, or municipal wastes (e.g. [66,67]). This hypothesis is supported by known anthropogenic contributions

to coastal northern Venezuela, including municipal and industrial wastes at reef sites [68] and elevated mollusk [69] and sedimentary [70] heavy metal concentrations near the Tuy, Tocuyo, and Aroa rivers. To test this hypothesis, Pb/Ca ratios were measured from the *M. annularis* core, observing three significant Pb/Ca maxima at 1932, 1940, and 1968 (Fig. 8). The third maximum is correlated with a 1969 Pb/Ca maximum observed from the Galápagos [71], suggesting this result might be of regional significance. Most importantly, the Pb/Ca results show no comparable mid-century reduction. Because anthropogenic cadmium and lead can be derived from separate sources (e.g. pigments versus gasoline additives), this observation cannot eliminate an anthropogenic cadmium artifact. The lack of a mid-century Pb/Ca transition, however, is consistent with the upwelling hypothesis.

3.4. Interdecadal trace element variability

Upwelling variability provides the best explanation for the trace element results given the limited Ba/Ca variability associated with the Cd/Ca reduction. This hypothesis is best tested by historical climate observations from the Cariaco Basin, including MAT and SST observations [13]. All three historical climate records show negative temperature anomalies from approximately 1920 to 1943, followed by positive temperature anomalies from 1943 to 1988 (Fig. 2). The raw Cariaco Basin SST anomalies also agree with the mean annual observations, with seven negative anomalies less than -3°C from 1920 to 1950 relative to two from 1950 to 1995³. These observations are in general agreement with the 1950 Cd/Ca reduction. Anomalously cool SSTs (-3.2°C) were observed at 1946, suggesting the inferred timing of the final 1946 Cd/Ca maximum is reasonable despite the apparent disagreement with the mean annual data. The potentially complex response of

mixed-layer cadmium concentrations to upwelling at the site is largely unknown, thus the trace element proxy records might not necessarily reflect a linear response to Cariaco Basin upwelling. A mid-century reduction in upwelling intensity, however, provides a consistent explanation for the trace element (Cd/Ca, Ba/Ca, and Pb/Ca) and historical climate records.

Can one link the inferred mid-20th century reduction in Cariaco Basin upwelling to a climate forcing mechanism? One possible mechanism is a northward meridional shift in ITCZ position (mean annual or seasonal), resulting in reduced trade wind intensity and elevated tropical North Atlantic SSTs. Both raw [13] and objectively analyzed [72] historical tropical North Atlantic SSTs were considered, calculating mean annual SST for the northern (5°N – 28°N , 70°W – 10°W) and southern (20°S – 5°N , 50°W – 10°E) tropical Atlantic (domains follow Servain [3]). Historical records from the tropical North Atlantic show a transition from anomalously cool to warm SSTs from 1925 to 1937 (data not shown), consistent with a decadal northward migration of the ITCZ approximately 10 years prior to the inferred change in Cariaco Basin upwelling. Either a significant lag is required to explain the tropical North Atlantic link, an additional forcing must be combined with the North Atlantic variability, or a separate mechanism is needed. The importance of tropical and subtropical North Atlantic forcing, however, should not be understated. From the COADS data set, correlation between Cariaco Basin historical SST (11°N , 65°W , 1859–1992) and the North Atlantic was calculated, shown in Fig. 10. Missing data from either the reference or target grid point were simply omitted from the calculation, and no interpolation or smoothing was utilized. Greatest correlation ($r > 0.7$) was observed for a large domain of the tropical–subtropical North Atlantic, increasing to $r > 0.8$ within the southern Caribbean (compare with figure 1 of Black et al. [7]). Thus historical Cariaco Basin variability is linked to the tropical North Atlantic on centennial time scales, but it cannot directly explain the inferred mid-century upwelling reduction.

ENSO forcing of the tropical North Atlantic

³ Aliasing by limited temperature observations would increase the possible number of winter SST anomaly events in the early section of this record. Neither record aliasing nor measurement bias ($< -0.49^{\circ}\text{C}$) can explain winter temperature anomalies in excess of -3°C .

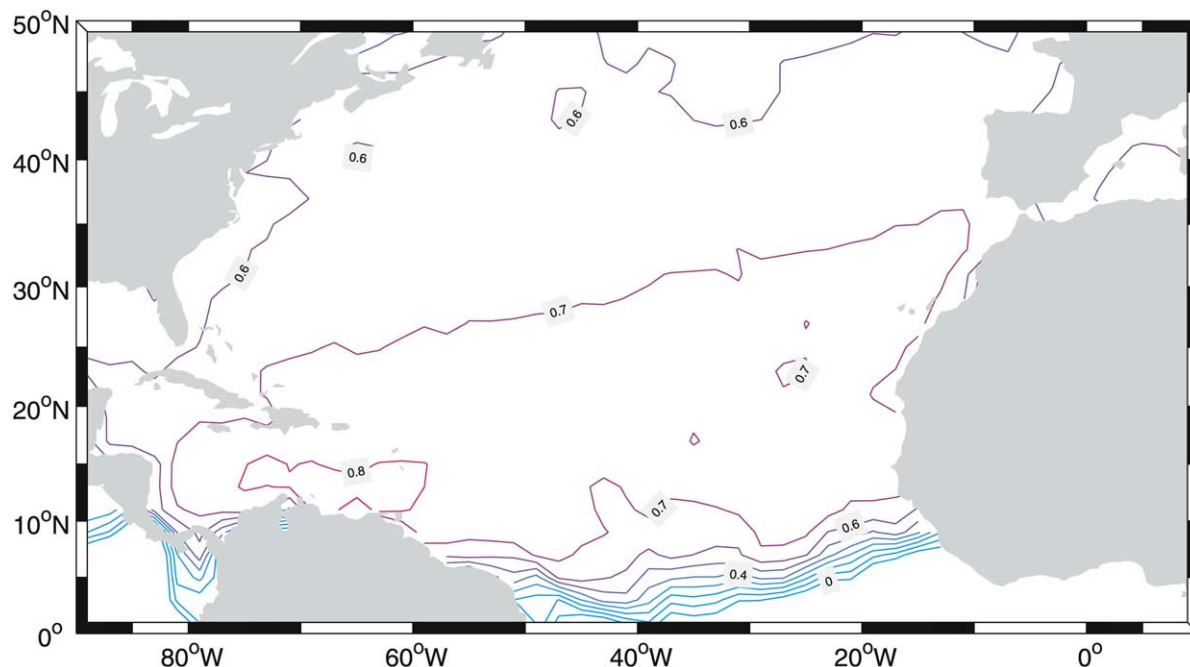


Fig. 10. Correlation map of Cariaco Basin historical SST. For each $2 \times 2^\circ$ cell, the correlation was calculated with respect to the 11°N , 65°W cell for the entire record (1859–1992). Historical SST data were taken from the COADS data set [13], and the contour map includes $r > 0$ at 0.1 intervals. As expected, greatest correlation is observed at cells adjacent to the 11°N , 65°W cell, and $r > 0.7$ is observed within the subtropical North Atlantic, tropical North Atlantic, and southern Caribbean. Historical SST data thus support a link between the Cariaco Basin and tropical–subtropical North Atlantic variability.

represents an alternative forcing mechanism for the Cariaco Basin region. As shown by Enfield and Mayer [56], the El Niño phase of the eastern equatorial Pacific is correlated with reduced northeasterly trade wind speed and persistent positive SST anomalies in the tropical North Atlantic (10 – 20°N , west of 40°W). A northward shift in the tropical Atlantic ITCZ thus results during the El Niño phase, and Enfield and Mayer [56] stated 50–80% of historical (1950–1992) tropical North Atlantic SST variability can be ascribed to ENSO variability. Although this mechanism might explain historical variability during the latter half of the 20th century, no comparable shift in ENSO indices (e.g. the Southern Oscillation Index or eastern equatorial Pacific SSTs; see Fedorov and Philander [73]) has occurred at 1950. The Cariaco Basin Ba/Ca record does show, however, consistently elevated Ba/Ca ratios from 1981 to 1995, in agreement with increased frequency of El Niño events and presumably linked to north-

ward ITCZ migration, enhanced precipitation over northern South America, and elevated fluvial discharge (increasing Cariaco Basin [Ba]). This preliminary observation, however, must be tested by cores taken directly within the Orinoco River discharge plume, not within the upwelling center of the Cariaco Basin. The trace element results suggest ENSO variability might have a significant effect on the hydrological cycle of the Cariaco Basin region, but a direct upwelling response is uncertain.

Considering this apparent shift in Cariaco Basin upwelling, to what extent does this interpretation agree with the sedimentary proxy records? The best comparison can be made with the decadal *G. bulloides* abundance record of Black et al. [7], where the relative and absolute abundances of this planktonic foraminifer from February to June have been correlated with upwelling intensity at this site [4], and references therein). As shown in Fig. 11, from 1920 to 1990 the trace element and

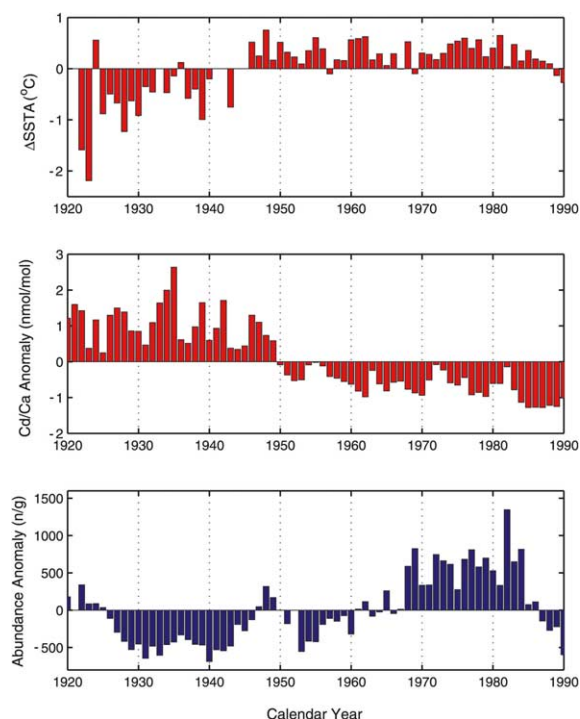


Fig. 11. Cariaco Basin proxy records and historical climate comparison. The upper two panels show the previously described mean annual Δ SSTA and Cd/Ca anomaly records from this site. The lower panel shows the *G. bulloides* faunal abundance data [7], core PL07-71BC. Note that the abundance minimum corresponds to the interval of coolest SSTs at this site.

faunal abundance records are inconsistent, with a greater correlation between Cd/Ca and mean annual SST relative to *G. bulloides* abundance. This observation does not necessarily refute the interpretation of Black et al. [7] given the significant correlation ($r=0.87$) between *G. bulloides* abundance and the tropical Atlantic SST gradient, but it suggests the nature of both geochemical and micropaleontological upwelling proxies at this site is more complicated than generally assumed.

Despite the general agreement between the historical climate records and the Cd/Ca results, these observations cannot provide a simple, linear interpretation of upwelling variations in this region. The Cd/Ca variability might be of local significance, resulting from island upwelling effects or local-scale cadmium sources, either natural or

anthropogenic. This local interpretation is supported by the tropical North Atlantic observations, including the zonal wind speed, interhemispheric SST anomalies, and North Atlantic SST anomalies (see figure 3 of [7]). This first interpretation, however, ignores multiple historical climate observations from this site, and a historical SST bias greater than 1°C is unlikely. Most importantly, false correlations result from comparing low-frequency signals within short time series records; the limited trace element observations presented here must be extended and replicated for a quantitative assessment.

4. Conclusions

In conclusion, the surface coral Cd/Ca and Ba/Ca records have raised several new questions regarding Cariaco Basin upwelling and its response to tropical Atlantic forcing. Three conclusions are obtained from these preliminary observations:

1. A two-fold reduction in the Cd/Ca ratio of *M. annularis* is observed from 1946 to 1952. No associated shift in the Ba/Ca ratio is apparent across this interval. This variability is consistent with the hydrographic distribution of cadmium and barium in the Cariaco Basin, suggesting a two-fold, centennial-scale reduction in upwelling intensity at this site.
2. Trace element artifacts are significant for surface coral records but do not mask the larger environmental variability. Both Cd/Ca and Ba/Ca ratios exhibit a kinetic dependence between *M. annularis* and *S. siderea*, with an approximate two-fold increase in elemental ratios associated with an equivalent reduction in annual extension rate. Anthropogenic variability at this site inferred from Pb/Ca ratios is also significant, with three maxima observed at 1932, 1940, and 1968. Kinetic and anthropogenic artifacts do not explain the mid-century Cd/Ca reduction.
3. The trace element variability agrees with historical climate observations from the Cariaco Basin, including absolute and relative historical SST and MAT records. The inferred upwelling reduction does not corroborate the faunal

abundance records from this region or the inferred North Atlantic extratropical forcing.

These results demonstrate the potential utility of combined geochemical and micropaleontological proxies from separate, annually resolved systems. The discrepant results between faunal abundance records, geochemical proxies, and the historical climate records suggest the response of these proxy systems to tropical upwelling is more complicated than generally assumed, requiring systematic modern calibrations. From the surface coral trace element records, past upwelling within the Cariaco Basin might therefore reflect a complex, non-linear system exhibiting centennial variability.

Acknowledgements

The laboratory assistance of Rick Kayser, Barry Grant, and Emmanuelle Puceat at MIT is gratefully acknowledged. Frank Urban, Christina Clark, and the officers and crew of the *Obsession* and *Doña Teresa* are thanked for their assistance in the field. Generous logistical and scientific support was also provided by the Estación de Investigaciones Marinas (EDIMAR), Fundación La Salle de Ciencias Naturales, Isla de Margarita, Venezuela. This work was supported by National Science Foundation Grant OCE-9510062 to J.E.C. and OCE-0002273 to E.A.B. M.K.R. is the recipient of a National Science Foundation Graduate Research Fellowship. **[BARD]**

References

- [1] C.K. Folland, T.N. Palmer, D.E. Parker, Sahel rainfall and worldwide sea surface temperatures, 1901–85, *Nature* 320 (1986) 602–606.
- [2] S. Hastenrath, Decadal-scale changes of the circulation in the tropical Atlantic sector associated with Sahel drought, *Int. J. Climatol.* 10 (1990) 459–472.
- [3] J. Servain, Simple climate indices for the tropical Atlantic Ocean and some applications, *J. Geophys. Res.* 96 (1991) 15137–15146.
- [4] L.C. Peterson, J.T. Overpeck, N.G. Kipp, J. Imbrie, A high-resolution late Quaternary upwelling record from the anoxic Cariaco Basin, Venezuela, *Paleoceanography* 6 (1991) 99–119.
- [5] P. Chang, L. Ji, H. Li, A decadal climate variation in the tropical Atlantic Ocean from thermodynamic air-sea interactions, *Nature* 385 (1997) 516–518.
- [6] K.A. Hughen, J.T. Overpeck, L.C. Peterson, R.F. Anderson, The nature of varved sedimentation in the Cariaco Basin, Venezuela, and its paleoclimatic significance, in: A.E.S. Kemp (Ed.), *Paleoclimatology and Paleoceanography from Laminated Sediments*, Geol. Soc. London, 1996.
- [7] D.E. Black, L.C. Peterson, J.T. Overpeck, A. Kaplan, M.N. Evans, M. Kashgarian, Eight centuries of North Atlantic ocean atmosphere variability, *Science* 286 (1999) 1709–1713.
- [8] G.H. Haug, K.A. Hughen, D.M. Sigman, L.C. Peterson, U. Röhl, Southward migration of the Intertropical Convergence Zone through the Holocene, *Science* 293 (2001) 1304–1308.
- [9] F.A. Richards, R.F. Vaccaro, The Cariaco Trench, an anaerobic basin in the Caribbean Sea, *Deep-Sea Res.* 3 (1956) 214–228.
- [10] K.A. Hughen, J.R. Southon, S.J. Lehman, J.T. Overpeck, Synchronous radiocarbon and climate shifts during the last deglaciation, *Science* 290 (2000) 1951–1954.
- [11] K.A. Hughen, J.T. Overpeck, S.J. Lehman, M. Kashgarian, J. Southon, L.C. Peterson, R. Alley, D.M. Sigman, Deglacial changes in ocean circulation from an extended radiocarbon calibration, *Nature* 391 (1998) 65–68.
- [12] H.L. Lin, L.C. Peterson, J.T. Overpeck, S.E. Trumbore, D.W. Murray, Late Quaternary climate change from $\delta^{18}\text{O}$ records of multiple species of planktonic foraminifera: High-resolution records from the anoxic Cariaco Basin, Venezuela, *Paleoceanography* 12 (1997) 415–427.
- [13] S.D. Woodruff, R.J. Slutz, R.L. Jenne, P.M. Steurer, A comprehensive ocean-atmosphere data set, *Bull. Am. Meteorol. Soc.* 68 (1987) 1239–1250.
- [14] P.D. Jones, T.M.L. Wigley, P.B. Wright, Global temperature variations between 1861 and 1984, *Nature* 322 (1986) 430–434.
- [15] G.T. Shen, E.A. Boyle, D.W. Lea, Cadmium in corals as a tracer of historical upwelling and industrial fallout, *Nature* 328 (1987) 794–796.
- [16] D.W. Lea, G.T. Shen, E.A. Boyle, Coralline barium records temporal variability in equatorial Pacific upwelling, *Nature* 340 (1989) 373–375.
- [17] G.T. Shen, T.M. Campbell, R.B. Dunbar, G.M. Wellington, M.W. Colgan, P.W. Glynn, Paleochemistry of manganese in corals from the Galapagos Islands, *Coral Reefs* 10 (1991) 91–100.
- [18] G.T. Shen, L.J. Linn, T.M. Campbell, A chemical indicator of trade wind reversal in corals from the western tropical Pacific, *J. Geophys. Res.* 97 (1992) 12689–12697.
- [19] G.R. Min, R.L. Edwards, F.R. Taylor, J. Recy, C.D. Gallup, J.W. Beck, Annual cycles of U/Ca in coral skeletons and U/Ca thermometry, *Geochim. Cosmochim. Acta* 59 (1995) 2025–2042.
- [20] G.T. Shen, R.B. Dunbar, Environmental controls on ura-

- nium in reef corals, *Geochim. Cosmochim. Acta* 59 (1995) 2009–2024.
- [21] E.R. Sholkovitz, G.T. Shen, The incorporation of rare earth elements in modern coral, *Geochim. Cosmochim. Acta* 59 (1995) 2749–2756.
- [22] G.T. Shen, J.E. Cole, D.W. Lea, L.J. Linn, T.A. McConaughy, R.G. Fairbanks, Surface ocean variability at Galapagos from 1936–1982: Calibration of geochemical tracers in corals, *Paleoceanography* 7 (1992) 563–588.
- [23] M.L. Delaney, L.J. Linn, E.R.M. Druffel, Seasonal cycles of manganese and cadmium in coral from the Galapagos Islands, *Geochim. Cosmochim. Acta* 57 (1993) 347–354.
- [24] L.M. Henderson, F.C. Kracek, The fractional precipitation of barium and radium chromates, *J. Am. Chem. Soc.* 49 (1927) 739–749.
- [25] S. de Villiers, G.T. Shen, B.K. Nelson, The Sr/Ca-temperature relationship in coralline aragonite: Influence of variability in $(\text{Sr}/\text{Ca})_{\text{seawater}}$ and skeletal growth parameters, *Geochim. Cosmochim. Acta* 58 (1994) 197–208.
- [26] S. de Villiers, B.K. Nelson, A.R. Chivas, Biological controls on coral Sr/Ca and $\delta^{18}\text{O}$ reconstructions of sea surface temperature, *Science* 269 (1995) 1247–1249.
- [27] M.K. Reuer, Centennial-scale elemental and isotopic variability in the tropical and subtropical North Atlantic Ocean, Ph.D. Thesis, MIT, 2002.
- [28] L. Jacobs, S. Emerson, S.S. Husted, Trace metal geochemistry in the Cariaco Trench, *Deep-Sea Res.* 34 (1987) 965–981.
- [29] K.K. Falkner, G.P. Klinkhammer, T.S. Bowers, J.F. Todd, B.L. Lewis, W.M. Landing, J.M. Edmond, The behavior of barium in anoxic marine waters, *Geochim. Cosmochim. Acta* 57 (1993) 537–554.
- [30] E.A. Boyle, J.M. Edmond, Copper in surface waters south of New Zealand, *Nature* 253 (1976) 107–109.
- [31] E.A. Boyle, S.S. Husted, S.P. Jones, On the distribution of copper, nickel, and cadmium in the surface waters of the North Atlantic and North Pacific Ocean, *J. Geophys. Res.* 86 (1981) 8048–8066.
- [32] L.H. Chan, D. Drummond, J.M. Edmond, B. Grant, On the barium data from the Atlantic GEOSECS Expedition, *Deep-Sea Res.* 24 (1977) 613–649.
- [33] F. Dehairs, R. Chesselet, J. Jedwab, Discrete suspended particles of barite and the barium cycle in the open ocean, *Earth Planet. Sci. Lett.* 49 (1980) 529–550.
- [34] J.K.B. Bishop, The barite-opal-organic carbon association in oceanic particulate matter, *Nature* 332 (1988) 341–343.
- [35] F.E. Müller-Karger, R. Varela, R. Thunell, M. Scranton, R. Bohrer, G. Taylor, J. Capelo, Y. Astor, E. Tappa, T.-Y. Ho, J.J. Walsh, Annual cycle of primary production in the Cariaco Basin: response to upwelling and implications for vertical export, *J. Geophys. Res.* 106 (2001) 4527–4542.
- [36] F.E. Müller-Karger, C.R. McClain, P.L. Richardson, The dispersal of the Amazon's water, *Nature* 333 (1988) 56–59.
- [37] F.E. Müller-Karger, Pigment distribution in the Caribbean Sea: Observations from space, *Prog. Oceanogr.* 23 (1989) 23–64.
- [38] H.T. Hochman, F.E. Müller-Karger, J.J. Walsh, Interpretation of the coastal zone color scanner signature of the Orinoco River plume, *J. Geophys. Res.* 99 (1994) 7443–7455.
- [39] J.M. Edmond, A. Spivack, B.C. Grant, H. Ming-Hui, C. Zexiam, C. Sung, Z. Xiushan, Chemical dynamics of the Changjiang estuary, *Cont. Shelf Res.* 4 (1985) 17–36.
- [40] A. Hernández-Guerra, T.M. Joyce, Water masses and circulation in the surface layers of the Caribbean at 66°W, *Geophys. Res. Lett.* 27 (2000) 3497–3500.
- [41] G.T. Shen, E.A. Boyle, Determination of lead, cadmium, and other trace metals in annually-banded corals, *Chem. Geol.* 97 (1988) 47–62.
- [42] E.A. Boyle, J.M. Edmond, Determination of trace metals in aqueous solution by APDC chelate co-precipitation, in: T.R.P. Gibb (Ed.), *Analytical Methods in Oceanography* 147, American Chemical Society, New York, 1975, pp. 44–55.
- [43] G.P. Klinkhammer, L.H. Chan, Determination of barium in marine waters by isotope dilution inductively coupled plasma mass spectrometry, *Anal. Chim. Acta* 232 (1990) 323–329.
- [44] J. Wu, E.A. Boyle, Low blank preconcentration technique for the determination of lead, copper, and cadmium in small-volume seawater samples by isotope dilution ICP-MS, *Anal. Chem.* 69 (1997) 2464–2470.
- [45] J.H. Hudson, E.A. Shinn, R.B. Halley, B. Lidz, Sclerochronology a tool for interpreting past environments, *Geology* 4 (1976) 361–364.
- [46] W.H.F. Smith, D.T. Sandwell, Global seafloor topography from satellite altimetry and ship depth soundings, *Science* 277 (1997) 1957–1962.
- [47] M.I. Scranton, F.L. Sayles, M.P. Bacon, P.G. Brewer, Temporal changes in the hydrography and chemistry of the Cariaco Trench, *Deep-Sea Res.* 34 (1987) 945–963.
- [48] S. Hastenrath, P.J. Lamb, *Climatic Atlas of the Tropical Atlantic and Eastern Pacific Oceans*, University of Wisconsin Press, Madison, WI, 1977.
- [49] T. Li, S.G.H. Philander, On the seasonal cycle of the equatorial Atlantic Ocean, *J. Clim.* 10 (1997) 813–817.
- [50] S. Curtis, S. Hastenrath, Forcing of anomalous sea surface temperature evolution in the tropical Atlantic during Pacific warm events, *J. Geophys. Res.* 100 (1995) 15835–15847.
- [51] P. Nobre, J. Shukla, Variations of sea surface temperature, wind stress, and rainfall over the tropical Atlantic and South America, *J. Clim.* 9 (1996) 2464–2479.
- [52] S.G.H. Philander, Why the ITCZ is mostly north of the equator, *J. Clim.* 9 (1996) 2958–2972.
- [53] S. Hastenrath, L. Greischar, Circulation mechanisms related to northeast Brazil rainfall anomalies, *J. Geophys. Res.* 98 (1993) 5093–5102.
- [54] A.D. Moura, J. Shukla, On the dynamics of droughts in northeast Brazil: Observations, theory, and numerical experiments with a general circulation model, *J. Atmos. Sci.* 38 (1981) 2657–2675.
- [55] R.W. Houghton, Y.M. Tourre, Characteristics of low-fre-

- quency sea surface temperature, *J. Clim.* 5 (1992) 765–771.
- [56] D.B. Enfield, D.A. Mayer, Tropical Atlantic sea surface temperature variability and its relation to El Niño–Southern Oscillation, *J. Geophys. Res.* 102 (1997) 929–945.
- [57] J.A. Carton, X. Cao, B.S. Giese, A.M. DaSilva, Decadal and interannual SST variability in the tropical Atlantic Ocean, *J. Phys. Oceanogr.* 26 (1996) 1165–1175.
- [58] D. Covey, S. Hastenrath, The Pacific El Niño phenomenon and the Atlantic circulation, *Mon. Weather Rev.* 106 (1978) 1280–1287.
- [59] S.E. Zebiak, Air–sea interaction in the equatorial Atlantic region, *J. Clim.* 6 (1993) 1567–1586.
- [60] J.A. Carton, B.H. Huang, Warm events in the tropical Atlantic, *J. Phys. Oceanogr.* 24 (1994) 888–903.
- [61] R. Kawamura, A rotated EOF analysis of global sea surface temperature variability with interannual and interdecadal scales, *J. Phys. Oceanogr.* 24 (1994) 707–715.
- [62] S. Hameed, K.R. Sperber, A. Meinster, Teleconnections of the Southern Oscillation in the tropical North Atlantic sector in the OSU coupled upper ocean atmosphere GCM, *J. Clim.* 6 (1993) 487–498.
- [63] G.T. Shen, Lead and cadmium geochemistry of corals: Reconstruction of historic perturbations in the upper ocean, Ph.D. Thesis, MIT, 1986.
- [64] M. Conkright, S. Levitus, T. Boyer, World Ocean Atlas 1994 Volume 1: Nutrients, U.S. Department of Commerce, Washington, DC, 1994.
- [65] A.L. Cohen, K.E. Owens, G.D. Layne, N. Shimizu, The effect of algal symbionts on the accuracy of Sr/Ca paleotemperatures from coral, *Science* 296 (2002) 331–333.
- [66] J.O. Nriagu, J.M. Pacyna, Quantitative assessment of worldwide contamination of air, water, and soils by trace metals, *Nature* 333 (1988) 134–139.
- [67] J.O. Nriagu, Global inventory of natural and anthropogenic emissions of trace metals to the atmosphere, *Nature* 279 (1979) 409–411.
- [68] M.P. Weiss, D.A. Goddard, Man's impact on coastal reefs - an example from Venezuela, in: M.P. Weiss, J.B. Saunders (Eds.), *Reefs and Related Carbonates - Ecology and Sedimentology*, AAPG, Tulsa, OK, 1977, pp. 171–179.
- [69] R. Jaffé, I. Leal, J. Alvarado, P. Gardinali, J. Sericano, Pollution effects of the Tuy River on the central Venezuelan coast: anthropogenic organic compounds and heavy metals in *Tivela mactroidea*, *Mar. Pollut. Bull.* 30 (1995) 820–825.
- [70] C. Bastidas, D. Bone, E.M. Garcia, Sedimentation rates and metal content of sediments in a Venezuelan coral reef, *Mar. Pollut. Bull.* 38 (1999) 16–24.
- [71] G.T. Shen, E.A. Boyle, Thermocline ventilation of anthropogenic lead in the western North Atlantic, *J. Geophys. Res.* 93 (1988) 15715–15732.
- [72] A. Kaplan, M. Cane, Y. Kushnir, A. Clement, M. Blumenthal, B. Rajagopalan, Analyses of global sea surface temperature 1856–1991, *J. Geophys. Res.* 103 (1998) 18567–18589.
- [73] A.V. Fedorov, S.G. Philander, Is El Niño changing?, *Science* 288 (2000) 1997–2002.
- [74] A. Da Silva, A.C. Young, S. Levitus, Atlas of Surface Marine Data, U.S. Department of Commerce, Washington, DC, 1994.
- [75] R.D. Shannon, Revised effective ionic radii and systematic studies of interatomic distances in halides and chalcogenides, *Acta Crystallogr. A* 32 (1976) 751–767.
- [76] S.R. Levitus, T.P. Boyer, World Ocean Atlas 1994, Volume 4: Temperature, U.S. Department of Commerce, Washington, DC, 1994.